

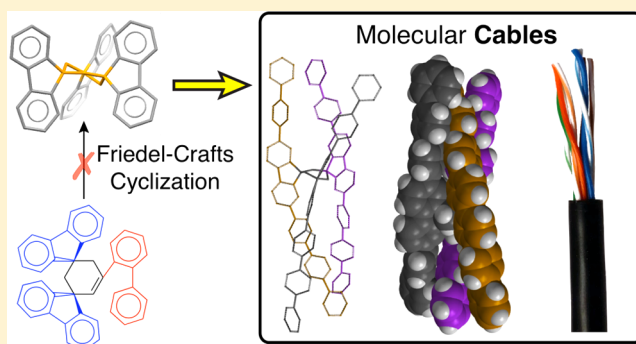
From Wires to Cables: Attempted Synthesis of 1,3,5-Trifluorenylcyclohexane as a Platform for Molecular Cables

Marat R. Talipov, Sameh H. Abdelwahed, Khushabu Thakur, Scott A. Reid,* and Rajendra Rathore*

Department of Chemistry, Marquette University, P.O. Box 1881, Milwaukee, Wisconsin 53201-1881, United States

S Supporting Information

ABSTRACT: Multiple molecular wires braided together in a single assembly, termed as molecular cable, are promising next-generation materials for effective long-range charge transport. As an example of the platform for constructing molecular cables, 1,3,5-trifluorenylcyclohexane (TFC) and its difluorenyl analogues (DFCs) were systematically investigated both experimentally (X-ray crystallography) and theoretically (DFT calculations). Although the syntheses of DFCs were successfully achieved, the synthesis of TFC, which involved a similar intramolecular Friedel–Crafts cyclization as the last step, was unsuccessful. An exhaustive study of the conformational landscape of cyclohexane ring of TFC and DFCs revealed that TFC is a moderately strained molecule (~17 kcal/mol), and computational studies of the reaction profile show that this steric strain, present in the transition state, is responsible for the unusually high (~5 years) reaction half-life. A successful synthesis of TFC will require that the steric strain is introduced in multiple steps, and such alternative strategies are being currently explored.



INTRODUCTION

Linearly connected polyfluorenes or ladder polyfluorenes¹ and poly-*p*-phenylenes^{2,3} have been extensively investigated as molecular wires for long-range charge transport.^{4–6} A cable is defined as two or more wires running side by side and bonded, twisted, or braided together to form a single assembly. We envisioned that 1,3,5-trifluorenylcyclohexane (TFC) could serve as a platform to construct molecular cables with three ladder polyfluorene or poly-*p*-phenylene wires braided together to allow effective electronic coupling (see Figure 1). Moreover, through-space electronic coupling among the braided poly-*p*-phenylene wires would be further facilitated via conformational transformations of the moderately strained cyclohexane ring (Figure 1).

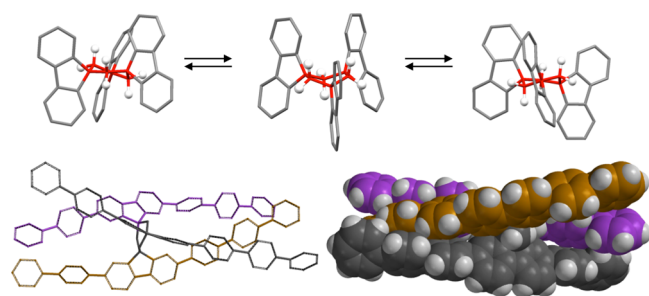
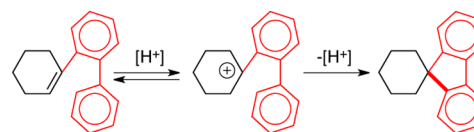


Figure 1. Conformational mobility of TFC and a representative example of AM1 minimized molecular cable shown as line and space-filling representations.

The intriguing conformational landscape of TFC and its promise for the preparation of next-generation charge-transport materials prompted us to design a straightforward 6-step synthesis based on well-known reactions (*vide infra*). However, the last step of this synthesis, an intramolecular Friedel–Crafts reaction to construct a fluorenylcyclohexane ring system

Scheme 1. Example of Intramolecular Friedel–Crafts Reaction to Construct Fluorenylcyclohexane Ring System

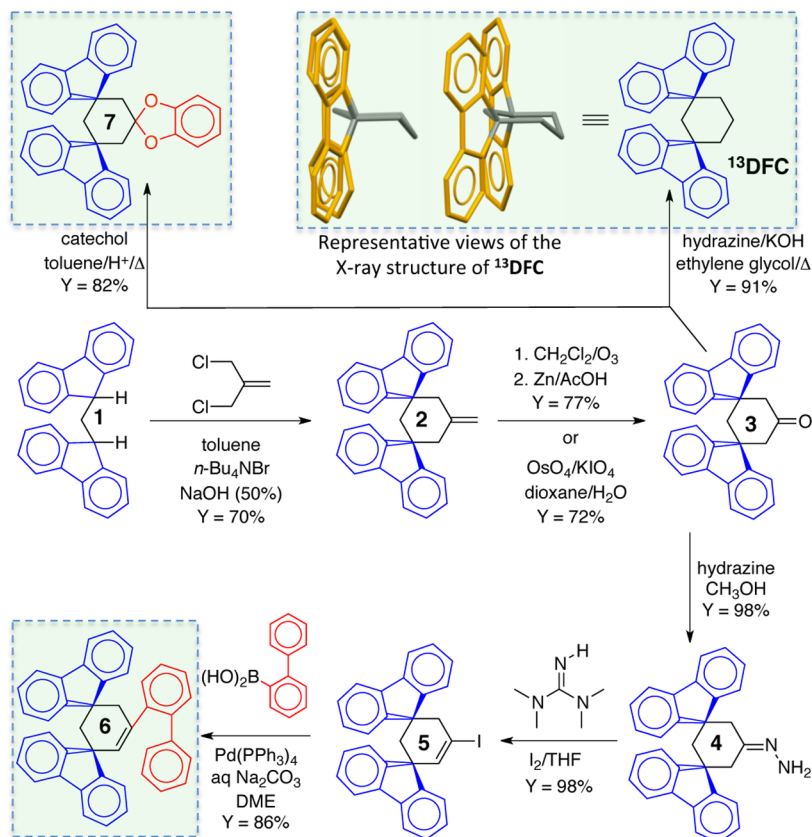


ample literature precedence,^{7,8} was unsuccessful. This is particularly curious, given that a successful synthesis of 1,4-difluorenylcyclohexane (¹⁴DFC) was carried out using a similar strategy.

To investigate this finding, we conducted and report herein a computational investigation using appropriately benchmarked DFT methods to elucidate the reasons behind failure of the intramolecular Friedel–Crafts ring closure to access TFC. These findings are further augmented by a careful mapping of the conformational space of ¹⁴DFC, 1,3-difluorenylcyclohexane (¹³DFC), and TFC by DFT calculations, which are compared

Received: December 9, 2015

Published: January 19, 2016

Scheme 2. Synthetic Route Towards the Preparation of Precursor of TFC and ^{13}DFC 

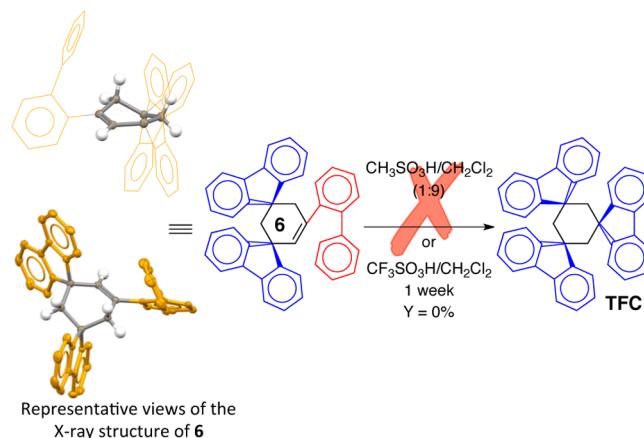
with experimental results from X-ray crystallography. A detailed computational analysis of the conformational landscape of TFC demonstrated that it is not an unreasonably strained molecule. However, analysis of the reaction profile and transition-state structure reveals that the key step of the multistep synthesis possesses a prohibitively high barrier, due to a combination of strained cyclohexane conformation and facial steric hindrance.

Despite the failure to access TFC, this study serves as a useful example of how an a priori computational analysis of key steps in synthetic designs of complex organic molecules can allow one to judiciously choose more facile routes while minimizing effort and resources on problematic strategies.

RESULTS AND DISCUSSION

A 6-step route for the synthesis of TFC is outlined in Schemes 2 and 3. The difluorenylmethane (1), readily available from a reaction of fluorene and formaldehyde with potassium *tert*-butoxide (KO^tBu) in DMF,⁷ was treated with 3-chloro-2-(chloromethyl)propene in DMF in the presence of KO^tBu to afford methylenecyclohexane 2 in ~70% yield. The methylenecyclohexane 2 can be converted to the corresponding cyclohexanone 3, either via ozonolysis in CH_2Cl_2 at -78°C (72% yield) or by a reaction with catalytic amounts of OsO_4 in the presence of potassium periodate in dioxane/ H_2O mixture (77% yield). The resulting cyclohexanone 3 was transformed to iodocyclohexene 5 in excellent yield by its conversion to the corresponding hydrazone 4, followed by a reaction with iodine in the presence of tetramethylguanidine as a base.⁹ The iodocyclohexene 5 was then subjected to Suzuki coupling reaction with 2-biphenylboronic acid in the presence of a palladium catalyst to afford 6—the Friedel–Crafts precursor to

Scheme 3. Attempted Acid-Catalysed Intramolecular Friedel–Crafts Cyclization of 6 to TFC and ORTEP Diagram of 6 (50% Probability)



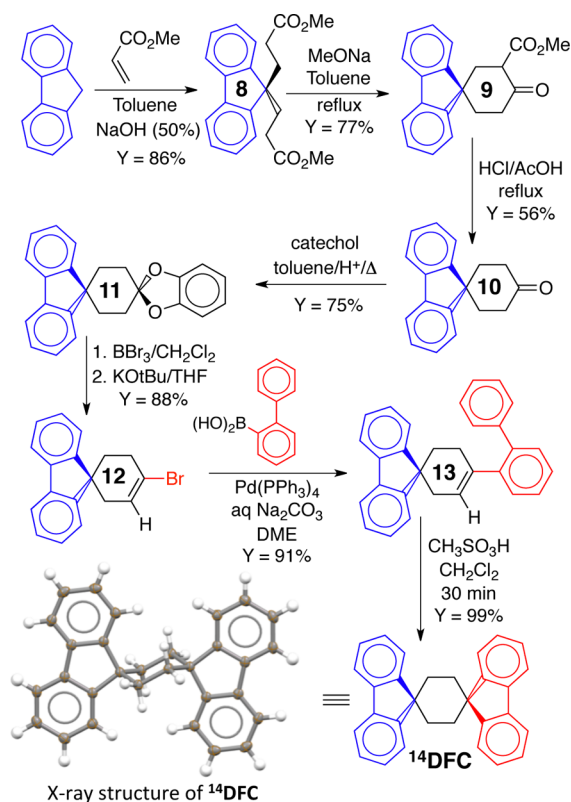
TFC—in excellent overall yield (see Scheme 2). The structure of 6 was confirmed by $^1\text{H}/^{13}\text{C}$ NMR spectroscopy, mass spectrometry, and by X-ray crystallography (Scheme 3). It is noted that the intermediate 3,5-difluorenylcyclohexanone 3 can be easily converted to the corresponding catechol ketal 7 or be reduced to ^{13}DFC , both in excellent yields (Scheme 2; also see the Supporting Information).

Subsequently, 6 was subjected to a Friedel–Crafts cyclization in a 9:1 (v/v) solution of CH_2Cl_2 and methanesulfonic acid (or trifluoromethanesulfonic acid), and stirring of the resulting reaction mixture was continued for an extended period (up to 1 week) at ambient temperature and under an argon atmosphere.

Although the color of the reaction mixture immediately darkened, the starting compound **6** was recovered quantitatively after aqueous workup. Treatment of **6** with polyphosphoric acid or concentrated sulfuric acid at 110 °C similarly did not afford TFC even after prolonged reaction times (>24 h), thereby attesting to its inertness toward the intramolecular Friedel–Crafts cyclization (Scheme 3; also see the Supporting Information).

This surprising observation of the inertness of **6** toward the intramolecular Friedel–Crafts cyclization prompted us to investigate the synthesis of another fluorenylcyclohexane derivative via the same route. Thus, the synthesis of ¹⁴DFC, a close analogue to TFC, outlined in Scheme 4, was successfully

Scheme 4. Successful Synthesis of ¹⁴DFC Using Acid-Catalyzed Intramolecular Friedel–Crafts Cyclization As the Key Synthetic Step and Its ORTEP Diagram (50% Probability)



achieved in excellent overall yield, and the critical synthetic step for its preparation is identical to the failed synthesis of TFC (Scheme 3) in all respects. Indeed, an intramolecular Friedel–Crafts cyclization of **13** (Scheme 4) in a 9:1 (v/v) solution of CH₂Cl₂ and methanesulfonic acid at ~0 °C for 30 min afforded crystalline ¹⁴DFC in quantitative yield. The structure of ¹⁴DFC was established by ¹H/¹³C NMR spectroscopy, mass spectrometry, and by X-ray crystallography (see Scheme 4; also see the Supporting Information).

The failure of intramolecular Friedel–Crafts cyclization of **6** to produce TFC, while the structurally similar **13** underwent a smooth Friedel–Crafts cyclization to ¹⁴DFC, prompted us to perform a detailed investigation of the mechanism of these transformations (i.e., Schemes 2–4). It is noteworthy that ¹³DFC and spirocatecholketal of 3,5-difluorenylcyclohexanone (i.e., **7**) can be easily prepared as stable molecules (Scheme 2);

and the failure of the synthesis of TFC suggests that the expected facial steric congestion by the three fluorenyl groups may be responsible for prohibiting intramolecular Friedel–Crafts ring closure. Accordingly, we sought to establish if TFC can exist as a stable molecule and undertook a systematic conformational analysis of TFC and ¹³DFC and ¹⁴DFC as well as the parent cyclohexane.

To cover the complete conformational space, we followed the Cremer–Pople approach, where all possible conformations of six-membered rings are mapped using three well-established cumulative puckering variables.¹⁰ These variables form a spherical coordinate set (Q , θ , and ϕ), where θ is the azimuthal angle ($\theta = 0–180^\circ$), ϕ is the polar angle ($\phi = 0–360^\circ$), and Q is the total puckering amplitude ($Q \geq 0$), which uniquely determines the position of each carbon atom in a cyclohexane ring on the z -coordinate (eq 1), i.e., its elevation/depression with respect to the mean plane $z = 0$ (see the Supporting Information for additional details).

$$z_j = \sqrt{\frac{1}{3}} Q \sin \theta \cos \left(\phi + \frac{2}{3} \pi [j - 1] \right) + \sqrt{\frac{1}{6}} Q \cos \theta (-1)^{j-1} \quad (1)$$

Combinations of the cumulative variables Q , θ , and ϕ generate all possible conformations of cyclohexane ring, and the positions of the typical conformations are identified on the sphere and its 2D map projection (see Figure 2). It is noted

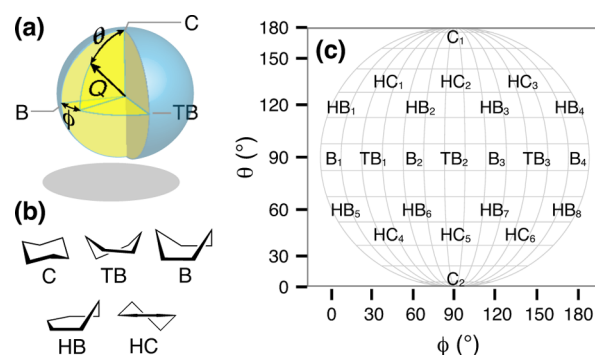


Figure 2. (a) Representation of spherical coordinates which were used to map the conformations of six-membered rings. (b) Typical conformations of cyclohexane ring and (c) their mapping to the (θ , ϕ) coordinates.

that only two variables (θ and ϕ) are needed to map every conformation in Figure 2, i.e. chair (C), twist-boat (TB), boat (B), half-boat (HB), and half-chair (HC, also known as twist-chair), at a fixed value of Q , which is essentially a measure of the displacement of the carbon atoms from the mean plane of cyclohexane ring. For example, a value of $Q = 0$ would produce a completely planar cyclohexane ring, *vide infra*.

Using the approach outlined in Figure 2, we computed the conformational landscape, and all resulting conformations were sequentially refined using molecular mechanics (UFF), semi-empirical (AM1), and DFT [M06-2X/6-31G(d)+PCM-(CH₂Cl₂)] calculations. The results are compiled in Figure 3 (also see Figure S5 in the Supporting Information for the corresponding AM1 plots).

First, conformational analysis of the parent cyclohexane with respect to θ and ϕ at a fixed Q reproduced all expected conformations. The chair conformer was the most stable one, while twist-boat and boat were 10.4 and 10.8 kcal/mol higher in energy (Figure 3a), with boat being the transition state between

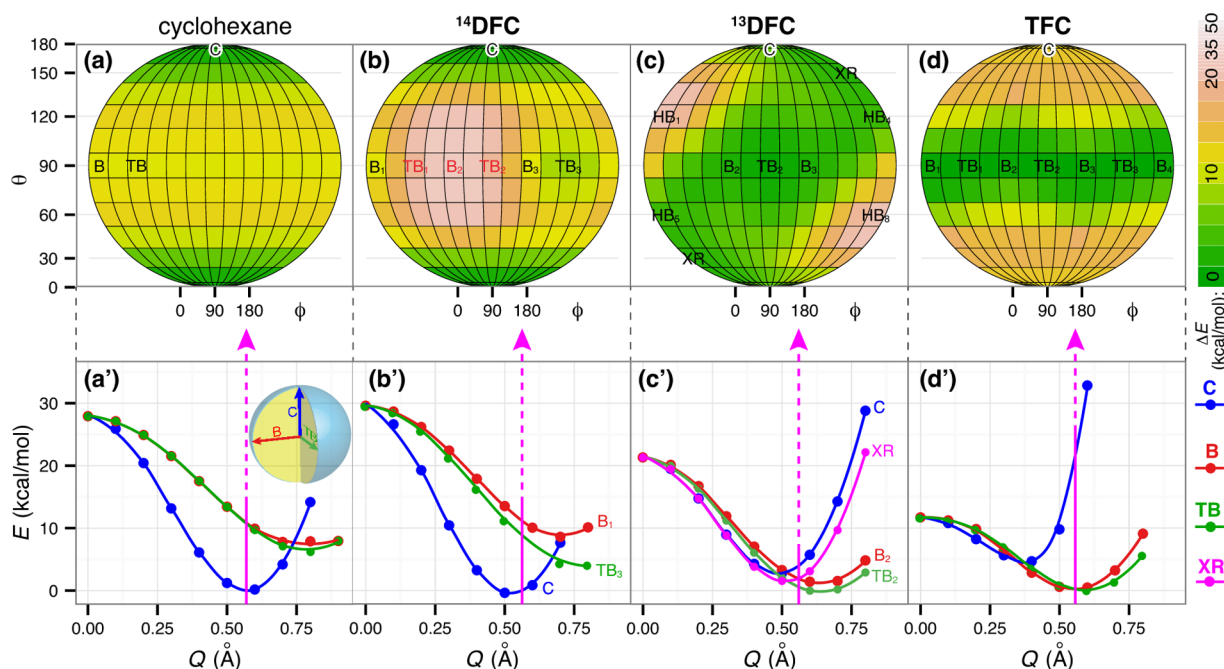


Figure 3. (a–d): Potential energy surface (PES) of cyclohexane, ¹⁴DFC, ¹³DFC, and TFC (as denoted on the plot) with respect to θ and ϕ at $Q = 0.57$ Å (Q was obtained from the DFT calculations of parent cyclohexane in its chair conformation [M06-2X/6-31G(d)+PCM(CH₂Cl₂)]. Step size of 15° was used for both θ and ϕ . Note that only one hemisphere of the conformational PES (i.e., for $\phi = 0$ –180°) is shown for brevity since the other hemisphere (i.e., for $\phi = 180$ –360°) is symmetrically identical to the shown part of the PES. (a'–d'): Potential energy of the most stable conformers [i.e., chair, boat, and half-boat-like (XR)] of cyclohexane, TFC, ¹³DFC, and ¹⁴DFC as a function of Q . Lines in panels (a'–d') were obtained by local polynomial regression fitting.

the enantiomeric twist-boat conformations. Importantly, in this scan (Figure 3a) the variable Q was fixed at the value of 0.57 Å, corresponding to a fully minimized chair conformation of cyclohexane. This value of Q does not necessarily correspond to an optimal value for other conformations; thus, we carried out another scan with respect to Q at fixed values of θ and ϕ for the most stable (identified) conformers: chair, boat, and twist-boat (Figure 3a'). Indeed, the lowest-energy boat and twist-boat conformers of cyclohexane occur at $Q = 0.8$ Å, and the resulting relative energies of the cyclohexane conformations [i.e., $\Delta E(B) = 6.2$ kcal/mol, $\Delta E(TB) = 7.8$ kcal/mol with respect to the chair conformer] were in close agreement with the well-accepted values of 5.5 and 6.9 kcal/mol for B and TB, respectively.^{11,12} As expected, all conformations converge to a planar structure [$\Delta E(P) = 27.9$ kcal/mol] when the value of Q is decreased to 0 Å.

A similar conformational scan of ¹⁴DFC with respect to θ and ϕ with $Q = 0.57$ Å (Figure 3b) identifies the chair as the most stable conformer, and its structure agrees well with experimental X-ray structure (Scheme 4). A number of different boat and twist-boat conformations are possible for ¹⁴DFC, because there are two sets of the opposing carbon atoms, with and without fluorenyl groups, which form the stern and bow of the boat. Expectedly, the boat and twist-boat conformations with fluorenyl-containing carbons forming the bow and stern of the boat lead to higher energy conformations due to increased steric effects [i.e., B₂ ($\Delta E = 26.7$ kcal/mol) and TB₁/TB₂ ($\Delta E = 18.8$ kcal/mol) conformations, see Figure 3b, also see Figure S6 in the Supporting Information]. At the same time, the energies of B and TB conformations without fluorene-containing bow-/stern-carbons [i.e., $\Delta E(B_1) = 10.9$ kcal/mol and $\Delta E(TB_3) = 8.3$ kcal/mol] are comparable to the parent cyclohexane (Figure 3 and Figure S6 in the Supporting

Information). A scan with respect to Q of the chair (C), boat (B₁), and twist-boat (TB₃) conformations of ¹⁴DFC showed that the value of Q for the lowest-energy conformations was similar (lower by ~ 0.1 Å) to the parent cyclohexane (compare Figure 3a',b').

For ¹³DFC, the situation is decidedly different. Here, the twist-boat conformation TB₂ was identified as the most stable conformer, while the chair (C) and boat (B₂) conformations were higher in energy by 4.4 and 1.7 kcal/mol, respectively, at $Q = 0.57$ Å (Figure 3c). The X-ray structure of ¹³DFC showed that its conformation (denoted XR) resembles a half-boat (Scheme 2). A number of half-boat conformations are possible for ¹³DFC. Higher energy half-boat conformations (e.g., HB₁/HB₈) are located at the northwestern (centered at $\theta = 105$ –150°, $\phi = 0$ °) and southeastern zones (centered at $\theta = 30$ –75°, $\phi = 180$ °) of the sphere and are 15–20 kcal/mol higher in energy than the most stable conformer TB₂ due to steric repulsion (Figure 3c, Figure S6 in the Supporting Information). The stable half-boat conformations (e.g., HB₄/HB₅), resembling the X-ray structure of ¹³DFC, were just 3.4 kcal/mol (at $Q = 0.57$ Å) higher in energy when compared with the most stable TB₂.

A scan of the most stable chair (C), boat (B₂), and twist-boat (TB₂) as well as half-boat-like (XR) conformations for ¹³DFC was performed with respect to Q and is displayed in Figure 3c'. Importantly, the lowest energy B₂, TB₂, and XR were found at a lower value of Q when compared to ¹⁴DFC, suggesting a flattening of the cyclohexane ring due to the presence of the 1,3-difluorenyl groups, see Figure 3c' and Figure S6 in the Supporting Information. The most stable twist-boat conformer (TB₂) and the half-boat-like conformation (XR) differed in energy only by 1.5 kcal/mol.¹³

With these computational observations in hand, we now turn to an analysis of the conformational landscape of TFC. Our calculations (Figure 3d) show that the low-energy conformations were all localized near the equator (i.e., $\theta = 90 \pm 15^\circ$). Considering that TB was the most stable conformer, the boat conformation, which constitutes a pseudorotational barrier between two TBs, was only 0.4 kcal/mol higher in energy (at $Q = 0.57 \text{ \AA}$), thus allowing a rapid interconversion of conformations along the equator (Figure 1). On the other hand, the chair conformation localized on the poles (C) was 12.0 kcal/mol higher in energy than TB, which can be readily attributed to the facial crowding among three fluorene fragments. In fact, such facial crowding can be dramatically reduced by flattening of the cyclohexane ring, i.e., by reducing Q from 0.57 to 0.4 \AA , the chair conformation was stabilized from $\Delta E(C) = 12.0$ to 4.6 kcal/mol (Figure 3d'). Furthermore, a completely planar cyclohexane ring in TFC (i.e., $Q = 0 \text{ \AA}$) is only 11.4 kcal/mol higher in energy than the most stable conformer TB (see Figure S6 in the Supporting Information).

The energetic penalty from facial crowding in TFC can be easily estimated as a sum of the strain energy of cyclohexane ring (E_{rs}) and steric repulsion among the fluorene fragments (E_{crowd}) based on the assumption that in a completely planarized TFC, the steric repulsion is negligible¹⁴ (Figure S6 in the Supporting Information). On this basis, the total energetic penalty in TFC can be evaluated as 17 kcal/mol, of which 7 kcal/mol arises directly from the facial crowding and 10 kcal/mol from the adaptation of cyclohexane ring from chair to twist-boat conformation and the considerable flattening of the ring (Figure 4).

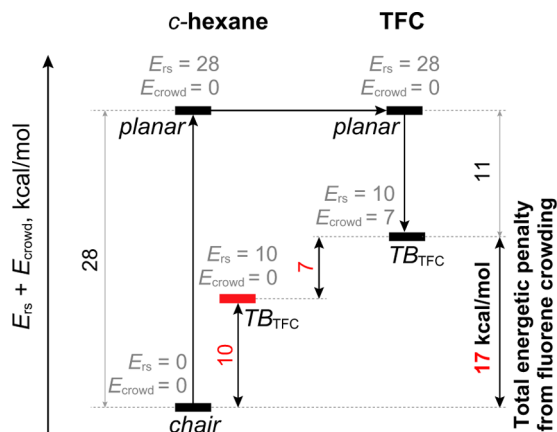


Figure 4. Evaluation of the total energetic penalty from fluorene crowding in TFC as a sum of the strain energy of cyclohexane ring (E_{rs}) and steric repulsion among the fluorene fragments (E_{crowd}) based on the assumption that $E_{crowd} = 0$ for completely planarized TFC [M06-2X/6-31G(d)+PCM(CH₂Cl₂)]. Note that $E_{rs} = 10$ kcal/mol for TB TFC was obtained from parent cyclohexane at the same coordinate set (Q , θ , and ϕ), which is shown as a red-colored bar. See Figure S7 in the Supporting Information for the extended version of the energy diagram including ¹⁴DFC and ¹³DFC.

The conformational analysis presented above clearly demonstrates that formation of TFC should be at least 17 kcal/mol more endothermic than the corresponding formation of ¹⁴DFC. To pinpoint how the endothermicity of formation of TFC affects its reaction rate, we computed the energetic profile for Friedel–Crafts cyclization of TFC, for which the attempted

synthesis was unsuccessful, and ¹⁴DFC, for which the corresponding cyclization proceeded smoothly (Figure 5).

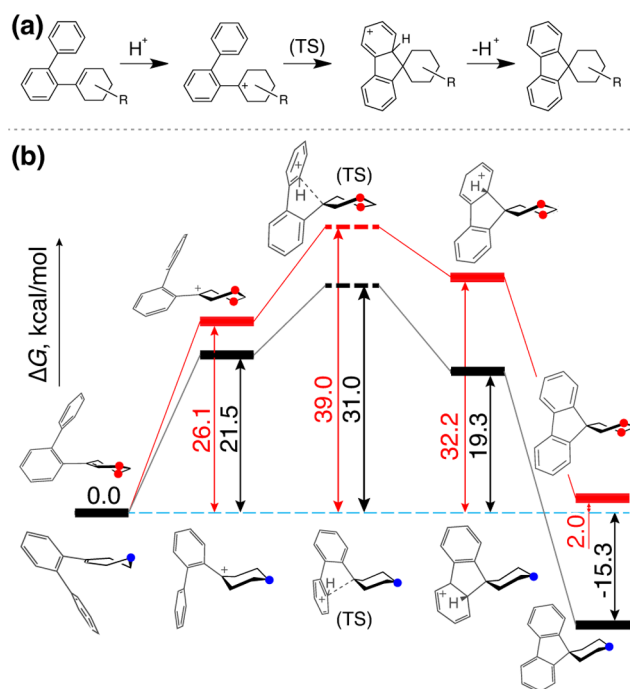


Figure 5. Mechanism (a) and the reaction profile [M06-2X/6-31G(d)+PCM(CH₂Cl₂)] (b) of formation of ¹⁴DFC and TFC via the intramolecular Friedel–Crafts cyclization. See also Figure S8 in the Supporting Information.

The key difference between the two reaction profiles in Figure 5 is the structure of the protonated intermediates (i.e., protonated starting olefin and product) and the transition states, which acquire twist-boat conformations in the case of TFC and chair conformations in the case of ¹⁴DFC. Thus, formation of TFC from **6** was almost thermoneutral ($\Delta G = 2.0$ kcal/mol), while formation of ¹⁴DFC from **13** was exothermic ($\Delta G = -15.3$ kcal/mol). Interestingly, the free energy changes for the formation of TFC and ¹⁴DFC differ by 17.3 kcal/mol (Figure 5), and this difference is in close agreement with the evaluated total steric strain in TFC of 17 kcal/mol when compared with unstrained cyclohexane (Figure 4). Moreover, the twist-boat conformation imposed by the facial crowding in TFC is preserved in its protonated form and the transition state. Accordingly, the net free activation energy of cyclization **6** \rightarrow TFC was 8 kcal/mol higher when compared to the cyclization **13** \rightarrow ¹⁴DFC. A simple estimation of the ratio between the reaction rates of formation of TFC and ¹⁴DFC at room temperature, based on the Eyring equation, showed that formation of TFC should be 5×10^6 times slower than that of ¹⁴DFC. Therefore, based on the observed half-life of 5 min for the transformation **13** \rightarrow ¹⁴DFC, the corresponding transformation **6** \rightarrow TFC would have a half-life of ~ 5 years (see the Supporting Information for details). Interestingly, lack of observation of any TFC in the attempted intramolecular Friedel–Crafts cyclization of **6** at 110 $^\circ\text{C}$, where the reaction is expected to be considerably faster, may indicate that this reaction is reversible, and the equilibrium favors the Friedel–Crafts precursor **6**.

CONCLUSIONS

In summary, TFC was envisioned as a platform to construct molecular cables with braided ladder polyfluorene or poly-*p*-phenylene wires. Straightforward synthetic strategies allowed ready preparation of ¹³DFC and ¹⁴DFC; however, synthesis of TFC, which involved a similar intramolecular Friedel–Crafts cyclization as the last step, was unsuccessful.

The results of the detailed conformational analysis of ¹⁴DFC, ¹³DFC, TFC, and parent cyclohexane, performed using DFT calculations and validated by the X-ray crystallography, showed that TFC is a relatively strained molecule (~17 kcal/mol) due to the facial crowding of fluorene fragments which leads to a considerable flattening of the twist-boat conformation. The calculated reaction profile of the transformation of the Friedel–Crafts precursor **6** to TFC showed that similar steric strain is also present in the transition state of the **6** → TFC transformation. By making use of the Eyring equation and the activation barrier from the reaction profile, it was clearly shown that the half-life of the reaction was prohibitively high (~5 years). At the same time, the **6** → TFC transformation is only slightly endothermic, $\Delta G(\mathbf{6} \rightarrow \mathbf{TFC}) = 2$ kcal/mol, and thus a successful synthesis of TFC is not prohibited from the thermodynamic consideration, thereby suggesting feasibility of designing an alternative synthetic route in which the strain energy is gradually introduced over multiple steps. A number of such strategies for the preparation of TFC are being currently explored.

EXPERIMENTAL SECTION

Preparation of 2. To a solution of difluorenylmethane **1** (5.0 g, 14.5 mmol) in toluene (200 mL) was successively added a solution of 50% NaOH (200 mL), 3-chloro-2-(chloromethyl)propene (1.5 mL, 14.5 mmol), and tetra-*n*-butylammonium bromide (100 mg) under an argon atmosphere and at 22 °C. The resulting mixture was stirred for 15 h, ethyl acetate (15 mL) was added, and the organic layer was separated. Aqueous layer was further extracted with ethyl acetate (2 × 30 mL), and the combined organic layers were washed with 5% hydrochloric acid (2 × 30 mL) and water (2 × 50 mL), dried over anhydrous MgSO₄, and evaporated under reduced pressure. The crude product was purified by column chromatography on silica gel using a 98:2 mixture of hexanes/ethyl acetate as eluent. Yield: 3.9 g, 70%; mp 152–154 °C; ¹H NMR (CDCl₃, 400 MHz) δ : 2.48 (s, 2H), 3.08 (s, 4H), 5.05 (s, 2H), 7.36–7.38 (m, 8 H), 7.64–7.66 (m, 4H), 7.71–7.73 (m, 4 H); ¹³C NMR (CDCl₃, 100 MHz) δ : 41.3, 43.3, 50.8, 113.7, 120.1, 124.0, 127.4, 127.9, 139.5, 142.3, 154.3. HRMS (APCI/IT-TOF) m/z : [M + H]⁺ calcd for C₃₁H₂₄ + H 397.1951; found 397.1941.

Preparation of 3. To a chilled (–78 °C) solution of **2** (3.5 g, 8.83 mmol) in dry CH₂Cl₂, ozone was bubbled for 45 min. Argon gas was then bubbled into the resulting blue solution until it became colorless. A mixture of zinc powder (6 g) and glacial acetic acid (15 mL) was added, and the resulting mixture was warmed to room temperature and stirred overnight. It was filtered through a short layer of Celite, and the filtrate was poured into water (50 mL). The organic layer was separated, and the aqueous layer was extracted with ethyl ether (3 × 40 mL). The combined organic extracts were washed with water, dried over anhydrous MgSO₄, and evaporated. Yield: 2.7 g, 77%; mp 148–150 °C (CH₂Cl₂/MeOH); ¹H NMR (CDCl₃, 400 MHz) δ : 2.74 (s, 2H), 3.13 (s, 4H), 7.36–7.39 (m, 8 H), 7.56 (m, 4H), 7.73 (m, 4 H); ¹³C NMR (CDCl₃, 100 MHz) δ : 43.4, 49.1, 50.7, 120.5, 123.4, 128.0, 128.4, 139.4, 153.2, 210.5. HRMS (APCI/IT-TOF) m/z : [M – 2H + H]⁺ calcd for C₃₀H₂₂O – 2H + H 397.1587; found 397.1580.

Alternative Preparation of 3. To a mixture of **2** (1.0 g, 2.5 mmol) and 2,6-lutidine (0.54 g, 5.0 mmol) dissolved in 3:1 mixture of dioxane and water (24 mL) was added a catalytic amount of OsO₄ (50 mg) followed by KIO₄ (2.31 g, 10.1 mmol). Resulting mixture was

then heated to reflux for 12 h. It was cooled to room temperature, diluted with water, and extracted with CH₂Cl₂ (3 × 25 mL). The combined organic extracts were washed with water (2 × 25 mL) and dried over MgSO₄. Evaporation of solvent under reduced pressure and column chromatography with a mixture of hexanes and ethyl acetate afforded 0.72 g (72%) of crystalline **3**.

Preparation of 5. Following closely a literature procedure,¹ finely powdered molecular sieves (6 g), methanol (30 mL), and hydrazine hydrate (3 mL) were added successively to a Schlenk flask, and the resulting mixture was stirred for 20 min. A methanol solution (50 mL) of the ketone (1.2 g, 3 mmol) was added dropwise to the above mixture, and it was stirred for 2 h. After which time, molecular sieves were filtered off and washed with CH₂Cl₂. The filtrate was evaporated in vacuo by gently heating to 30–40 °C to afford hydrazone **4** in excellent yield 1.22 g (98%); mp 220–222 °C; (CH₂Cl₂/MeOH); ¹H NMR (CDCl₃, 400 MHz) δ : 2.61 (s, 2H), 2.97 (s, 2H), 3.11 (s, 2H), 5.05 (s, 2H), 7.32–7.42 (m, 9H), 7.66–7.68 (m, 7H). Note that the hydrazone **4** was used in the next step without further purification.

To a solution of *N,N,N',N'*-tetramethylguanidine (1.25 mL, 9.8 mmol) and THF (15 mL) was slowly added during 30 min a solution of iodine (1.24 g, 4.9 mmol) in THF (15 mL) at 0 °C.² To the resulting mixture was added dropwise a solution of crude hydrazone (0.4 g, 0.98 mmol), from the previous reaction, in THF (30 mL) over 10 min at 0 °C. The reaction was instantaneous, but the stirring was continued for an additional 15 min. The reaction mixture was washed with 5% HCl, aqueous Na₂SO₃, and aqueous NaHCO₃ and dried over MgSO₄. After removal of the solvent under reduced pressure, the residue was subjected for a flash column chromatography using silica gel and hexanes/ethyl acetate (98:2) as the eluent to give the title compound **5**. Yield: 0.49 g (98%); mp 284–286 °C (CH₂Cl₂/MeOH); ¹H NMR (CDCl₃, 400 MHz) δ : 2.66 (s, 2H), 3.19 (s, 2H), 6.37 (s, 1H), 7.21–7.41 (m, 8 H), 7.55–7.73 (m, 8 H); ¹³C NMR (CDCl₃, 100 MHz) δ : 43.2, 48.0, 52.0, 57.3, 94.3, 120.3, 120.6, 125.0, 125.2, 127.9, 128.1, 128.3, 128.6, 140.1, 140.1, 142.9, 151.73, 152.67. HRMS (APCI/IT-TOF) m/z : [M + H]⁺ calcd for C₃₀H₂₁I + H 509.0761; found 509.0765.

Preparation of 6. Biphenyl-2-boronic acid (0.26 g, 1.33 mmol) and iodo derivative **5** (0.45 g, 0.89 mmol) were added to a solution of tetrakis(triphenylphosphine)palladium(0) (50 mg) in 1,2-dimethoxyethane (50 mL) at 22 °C and under an argon atmosphere. To this stirred mixture was added 4 M aqueous sodium carbonate (15 mL), and then the reaction mixture was refluxed for 12 h. It was then poured onto water (40 mL), and the resulting aqueous layer was extracted with CH₂Cl₂ (3 × 25 mL). The organic layers were combined, dried over magnesium sulfate, and evaporated. The resulting crude product was chromatographed over silica gel using 98:2 mixture of hexanes/ethyl acetate to afford pure **6** as a white crystalline solid. Yield: 0.4 g (86%); mp 292–294 °C (CH₂Cl₂/MeOH); ¹H NMR (CDCl₃, 400 MHz) δ : 2.32 (s, 2H), 2.63 (s, 2H), 5.88 (s, 1H), 7.18–7.76 (m, 25 H); ¹³C NMR (CDCl₃, 100 MHz) δ : 38.1, 42.5, 49.0, 52.6, 118.8, 118.9, 123.4, 123.8, 125.9, 126.05, 126.10, 126.2, 126.4, 126.8, 127.1, 127.7, 128.5, 129.1, 138.2, 138.6, 138.7, 139.2, 141.4, 141.9, 151.5, 153.3. HRMS (APCI/IT-TOF) m/z : [M + H]⁺ calcd for C₄₂H₃₀ + H 535.2420; found 535.2420.

Preparation of 7. To a solution of catechol (0.44 g, 4 mmol) and 3,5-difluoranyl cyclohexanone **3** (0.80 g, ~2 mmol) in toluene (60 mL) was added a catalytic amount of *p*-toluenesulfonic acid (50 mg), and the flask was outfitted with Dean–Stark trap. The mixture was refluxed overnight, and the water was separated in the Dean–Stark trap. After cooling, the reaction mixture was washed with 5% aqueous NaHCO₃ (2 × 30 mL) and water (2 × 30 mL). After evaporation of the solvent, the crude product was chromatographed on silica gel using hexanes/ethyl acetate (90:10) mixture as the eluent to afford the ketal **7** as a white solid. Yield: 0.9 g (82%); mp 224–226 °C (CH₂Cl₂/MeOH); ¹H NMR (CDCl₃, 400 MHz) δ : 2.62 (s, 2H), 2.95 (s, 4H), 6.73 (s, 4H), 7.36–7.46 (m, 8H), 7.74 (m, 4H), 7.85 (m, 4H); ¹³C NMR (CDCl₃, 100 MHz) δ : 43.5, 44.9, 49.9, 108.7, 118.1, 120.1, 121.3, 124.7, 127.7, 128.0, 140.0, 146.9, 153.3. HRMS (APCI/IT-TOF) m/z : [M – 2H + H]⁺ calcd for C₃₆H₂₆O₂ – 2H + H 489.1849; found 489.1840.

Preparation of ¹³DFC. In a Schlenk flask under argon ketone **3** (250 mg, 0.627 mmol) was dissolved in ethylene glycol (10 mL). Hydrazine hydrate (554 mg, 9.41 mmol) was added to reaction mixture and stirred for 10 min, followed by addition of KOH (527 mg, 9.41 mmol). Reaction mixture was then heated to reflux over 5 h. After that, the reaction mixture was cooled to room temperature and diluted with 37% HCl. Mixture was extracted with dichloromethane and washed with water. Organic layer was dried over MgSO₄ and evaporated under reduced pressure. Crude product was then passed through short pad of silica and recrystallized from dichloromethane and methanol to yield 91% of pure ¹³DFC; mp 170–172 °C (CH₂Cl₂/MeOH); ¹H NMR (CDCl₃, 400 MHz): 7.74(m, 8H), 7.37(m, 8H), 2.46(s, 2H), 2.29(s, 6H); ¹³C NMR (CDCl₃, 100 MHz): 17.6, 32.2, 42.6, 50.5, 120.1, 124.2, 127.2, 127.8, 139.6, 155.1. HRMS (APCI/IT-TOF) *m/z*: [M + H]⁺ calcd for C₃₀H₂₄ + H 385.1951; found 385.1950.

Synthesis of Spiro[cyclohexane-1,9'-fluoren]-4-one (10). Three-step synthesis of cyclohexanone **10** was accomplished closely following the literature procedures,^{3,4} and the ¹H/¹³C data matched well with the reported data. ¹H NMR (CDCl₃, 400 MHz) δ 2.19 (t, 4H), 2.85 (t, 4H), 7.34 (t, 2H), 7.43 (t, 2H), 7.60 (d, 2H), 7.80 (d, 2H); ¹³C NMR (CDCl₃, 100 MHz) δ 35.7, 39.1, 49.0, 120.4, 123.8, 127.5, 127.8, 139.9, 150.9, 211.5.

Synthesis of 11. To a solution of catechol (6.2 g, 56 mmol) and **10** (9.2 g, 37 mmol) in toluene (100 mL) was added a catalytic amount of *p*-toluenesulfonic acid (0.1 g), and the flask was outfitted with Dean–Stark trap. The mixture was stirred at refluxing temperature for overnight, and the water was separated from the reaction system by azeotropic distillation with a water separator using Dean–Stark trap. After cooling, the reaction mixture was washed with water (3 × 30 mL). After evaporation of the solvent, the crude products were chromatographed on silica gel and eluted with hexane/ethyl acetate (96:4) as the eluent to give the ketal **11** as a white solid. Yield: 9.5 g (75%); mp 215–217 °C; (CH₂Cl₂/MeOH); ¹H NMR (CDCl₃, 400 MHz) δ 2.09 (t, 4H), 2.45 (t, 4H), 6.85 (d, 4H), 7.32–7.43 (m, 4H), 7.70 (d, 2H), 7.77 (2, 2H); ¹³C NMR (CDCl₃, 100 MHz) δ 32.8, 33.2, 49.3, 109.3, 118.2, 120.6, 121.7, 124.6, 127.7, 127.9, 140.3, 147.8, 152.0. HRMS (APCI/IT-TOF) *m/z*: [M – 2H + H]⁺ calcd for C₂₄H₂₀O₂ – 2H + H 339.1380; found 339.1370.

Preparation of 12. To a magnetically stirred solution of the spirocatechol ketal (5.0 g, 14.7 mmol) in dichloromethane (30 mL), cooled in an ice-salt bath, was added dropwise a 1 M solution of boron tribromide in dichloromethane (20 mL, 20 mmol) under an argon atmosphere. The resulting mixture was stirred for 8 h at 0 °C, and after which time it was quenched with ice-cold water (50 mL), and the dichloromethane layer was separated. The aqueous layer was extracted with dichloromethane (3 × 25 mL). The combined organic extracts were washed successively with water (50 mL), 10% sodium hydroxide (2 × 25 mL), and water (50 mL) and then dried over anhydrous magnesium sulfate. Evaporation of the solvent and filtration through a pad of silica gel hexane/ethyl acetate (98:2) as the eluent afforded the *gem*-dibromide as the pure product. Yield: 5.4 g (94%); mp 165–167 °C; (CH₂Cl₂/MeOH); ¹H NMR (CDCl₃, 400 MHz) δ: 1.97 (br s, 4H), 2.98 (t, 4H), 7.31–7.43 (m, 4H), 7.61 (d, 2H), 7.75 (d, 2H); ¹³C NMR (CDCl₃, 100 MHz) δ 34.4, 46.5, 48.4, 70.9, 120.4, 124.8, 127.6, 127.8. This *gem*-dibromide was used in the next step without further characterization.

To a magnetically stirred solution of *gem*-dibromide (5.4 g, 13.77 mmol), obtained above, in anhydrous THF (60 mL) was added excess potassium *tert*-butoxide (2.8 g, 24.78 mmol). The resulting mixture was stirred under an argon atmosphere for 3 h at 22 °C. The reaction was quenched with saturated ammonium chloride solution (50 mL) and triturated with dichloromethane (100 mL). The organic layer was separated, and the aqueous layer was further extracted with dichloromethane (3 × 25 mL). Combined organic extracts were washed with water (3 × 25 mL) and brine (3 × 25 mL) and dried over anhydrous magnesium sulfate. Evaporation of the solvent gave the crude material which was purified by column chromatography using a 98:2 mixture of hexanes/ethyl acetate as eluent to afford **12** the pure product. Yield: 4.0 g (93%); mp 160–162 °C; ¹H NMR (CDCl₃, 300

400 MHz) δ: 1.92 (t, 2H), 2.48 (m, 2H), 2.83 (m, 2H), 6.34 (m, 1H), 7.30–7.47 (m, 6H), 7.57 (d, 2H); ¹³C NMR (CDCl₃, 300 MHz) δ: 34.051, 34.22, 36.859, 47.30, 120.13, 122.273, 123.394, 127.62, 127.657, 128.61, 139.78, 151.475. HRMS (APCI/IT-TOF) *m/z*: [M – H + H]⁺ calcd for C₁₈H₁₃Br – H + H 310.0352; found 310.0350.

Preparation of 13. A freshly prepared solution of 2-biphenylmagnesium bromide [from 2-bromobiphenyl (3.7 mL, 21.4 mmol) and excess magnesium turnings (1.03 g, 42.92 mmol) in anhydrous THF (50 mL)] was transferred to a Schlenk flask containing **12** (3.8 g, 12.2 mmol) and a catalytic amount of bis(triphenylphosphine)palladium dichloride (0.1 g) under an argon atmosphere and at 22 °C. The resulting yellow mixture was refluxed for overnight, cooled to room temperature, and quenched with saturated ammonium chloride solution (50 mL). The aqueous layer was extracted with dichloromethane (3 × 50 mL), and the combined organic extracts were dried over anhydrous magnesium sulfate and filtered. Evaporation of the solvent in vacuo afforded the crude material which was subjected to flash chromatography on silica gel, eluted with hexane as the eluent to give a white solid. Yield: 4.1 g (88%); mp 174–176 °C; (CH₂Cl₂/MeOH); ¹H NMR (CDCl₃, 400 MHz) δ: 1.58 (t, 2H), 2.19 (t, 2H), 2.48 (d, 2H), 5.99 (m, 1H), 7.20–7.51 (m, 15H), 7.67 (d, 2H); ¹³C NMR (CDCl₃, 100 MHz) δ: 28.2, 31.1, 35.1, 47.8, 119.9, 123.8, 127.1, 127.15, 127.23, 127.26, 127.34, 127.58, 128.3, 129.3, 129.6, 130.5, 139.5, 139.7, 140.3, 152.7. HRMS (APCI/IT-TOF) *m/z*: [M + H]⁺ calcd for C₃₀H₂₄ + H 385.1951; found 385.1950.

Alternative Preparation of 13. A mixture of biphenyl-2-boronic acid (2.4 g, 12 mmol) and **12** (3.04 g, 10 mmol) was added to a solution of tetrakis(triphenylphosphine)palladium (100 mg) in 1,2-dimethoxyethane (100 mL) at 22 °C and under an argon atmosphere. To this stirred mixture was added 4 M aqueous sodium carbonate (40 mL), and the resulting mixture was refluxed for 16 h. It was then poured onto water (200 mL), and the aqueous layer was extracted with CH₂Cl₂ (3 × 50 mL). The organic layers were combined, dried over magnesium sulfate, and evaporated. The resulting crude product was chromatographed over silica gel using 98:2 mixture of hexanes/ethyl acetate to afford pure **13** as a white crystalline solid. Yield: 3.5 g (91%).

Preparation of ¹⁴DFC. The compound **13** (1.9 g, 5 mmol) was dissolved in 50 mL of dry dichloromethane and cooled to 0 °C, and then methanesulfonic acid (5 mL) was added dropwise to the solution. The resulting mixture was allowed to stir at room temperature for 30 min and then quenched with aqueous NaHCO₃ (100 mL, 10%). The organic layer was separated, washed with water, and dried over MgSO₄. Evaporation of the solvent in vacuo and crystallization from a mixture of dichloromethane and methanol afforded pure ¹⁴DFC. Yield: 1.88 g (99%); mp 286–288 °C; (CH₂Cl₂/MeOH); ¹H NMR (CDCl₃, 400 MHz) δ: 2.28 (br s, 8H), 7.44–7.47 (m, 8H), 7.82–7.85 (m, 4H), 8.00–8.03 (m, 4H); ¹³C NMR (CDCl₃, 100 MHz) δ 32.7, 49.9, 120.6, 124.6, 127.6, 127.8, 140.3, 153.4. HRMS (APCI/IT-TOF) *m/z*: [M + H]⁺ calcd for C₃₀H₂₄ + H 385.1951; found 385.1950.

■ ASSOCIATED CONTENT

📄 Supporting Information

The Supporting Information is available free of charge on the ACS Publications website at DOI: 10.1021/acs.joc.5b02792.

¹H and ¹³C NMR spectra; computational details; the coordinates and energies of the calculated structures; and Figures S1–S8 and Tables S1–S4. Note that crystal structures were also deposited at the Cambridge Crystallographic Data Centre with the deposition numbers CCDC 1420779, 1420780, and 1420781 (PDF)

Crystallographic data (CIF)

Crystallographic data (CIF)

Crystallographic data (CIF)

Crystallographic data (CIF)

AUTHOR INFORMATION

Corresponding Authors

*E-mail: scott.reid@marquette.edu.

*E-mail: rajendra.rathore@marquette.edu.

Notes

The authors declare no competing financial interest.

ACKNOWLEDGMENTS

We thank the NSF (CHE-1508677) and NIH (R01-HL112639-04) for financial support, Dr. Sergey V. Lindeman for X-ray crystallography, and Professor Q. K. Timerghazin for helpful discussions. The calculations were performed on the high-performance computing cluster Pèrè at Marquette University funded by NSF awards OCI-0923037 and CBET-0521602, and the Extreme Science and Engineering Discovery Environment (XSEDE) funded by NSF (TG-CHE130101).

REFERENCES

- (1) Scherf, U.; Neher, D. *Polyfluorenes*; Springer: New York, 2008.
- (2) Banerjee, M.; Shukla, R.; Rathore, R. *J. Am. Chem. Soc.* **2009**, *131*, 1780–1786.
- (3) Talipov, M. R.; Boddada, A.; Timerghazin, Q. K.; Rathore, R. *J. Phys. Chem. C* **2014**, *118*, 21400–21408.
- (4) Weiss, E. A.; Ahrens, M. J.; Sinks, L. E.; Gusev, A. V.; Ratner, M. A.; Wasielewski, M. R. *J. Am. Chem. Soc.* **2004**, *126*, 5577–5584.
- (5) James, D. K.; Tour, J. M. *Top. Curr. Chem.* **2005**, *257*, 33–62.
- (6) Weiss, E. A.; Tauber, M. J.; Kelley, R. F.; Ahrens, M. J.; Ratner, M. A.; Wasielewski, M. R. *J. Am. Chem. Soc.* **2005**, *127*, 11842–11850.
- (7) Rathore, R.; Abdelwahed, S. H.; Guzei, I. A. *J. Am. Chem. Soc.* **2003**, *125*, 8712–8713.
- (8) Vura-Weis, J.; Abdelwahed, S. H.; Shukla, R.; Rathore, R.; Ratner, M. A.; Wasielewski, M. R. *Science* **2010**, *328*, 1547–1550.
- (9) Barton, D. H.; Bashiardes, G.; Fourrey, J.-L. *Tetrahedron* **1988**, *44*, 147–162.
- (10) Cremer, D. T.; Pople, J. A. *J. Am. Chem. Soc.* **1975**, *97*, 1354–1358.
- (11) Anslyn, E. V.; Dougherty, D. A. *Modern physical organic chemistry*; University Science: Sausalito, CA, 2006.
- (12) Wade, L. G. *Organic chemistry*; Pearson: Boston, 2013.
- (13) This difference is not surprising in the light of the fact that a comparison is being made between the solid-state X-ray structure prone to packing forces and computed solution structure.
- (14) Lack of fluorene–fluorene repulsion in TFC with planarized cyclohexane ring can be confirmed by the thermal neutrality (within the chemical accuracy of 1 kcal/mol) of homodesmic reactions, in which cyclohexane ring was kept planarized: $^{14}\text{DFC} \rightarrow ^{13}\text{DFC}$ ($\Delta E = 0.4$ kcal/mol) and $^{13}\text{DFC} \rightarrow 2/3 \text{ TFC} + 1/3 \text{ cyclohexane}$ ($\Delta E = 0.8$ kcal/mol).